Transfer function models for using empirical and physics-based simulation signal response data

Ajay M. Koshti
NASA Johnson Space Center, Houston, U. S. A.

ABSTRACT

In many situations, real or induced flaws such as tight cracks with known morphology cannot be manufactured in part geometry specimens or in real parts. Typically, surface fatigue cracks are manufactured in simple geometry specimens such as flat plates, dog-bone shaped flat or cylindrical specimens. If a nondestructive evaluation (NDE) technique is required to provide a reliably detectable flaw size, denoted as $a_{90/95}$, for induced flaws in a part, then a direct method for qualifying the NDE procedure is to use appropriate induced flaw specimens and perform NDE procedure demonstration on the specimens. Probability of detection (POD) analysis of the empirical data may provide estimation of $a_{90/95}$. This approach is described as direct POD demonstration testing, which may follow guidelines of MIL-HDBK-1823. This paper considers a case, where embedded tight cracklike induced flaws are to be detected reliably using a signal response based NDE procedure. Here, it is assumed that it is not practical to make surface or embedded induced flaw specimens in part geometry or configuration. Therefore, a direct POD demonstration testing cannot be undertaken. It is also assumed that simulation of signal response is possible for both surface and embedded induced flaws in part geometry specimens using a physics-based model. The proposed approach for NDE procedure qualification uses artificial flaws in simple geometry and part geometry specimens, and induced flaws in the same type of simple geometry specimens. Signal response data is taken on all sets of artificial and induced flaws in simple geometry and part geometry specimens. Moreover, simulated signal response data is generated for surface and embedded flaws. Thus, a case of five signal response versus flaw size datasets is considered. Three of the datasets are empirical and two datasets are physics model-based simulation datasets. A method of devising and using transfer function calculation dataset blocks to estimate the either the reliably detectable flaw size or the demonstration flaw size is provided.

Keywords: Nondestructive evaluation, probability of detection, transfer function

1. INTRODUCTION

Since, transfer function relates to probability of detection (POD), first key references in POD and relevant transfer function references are mentioned in this section. MIL-HDBK-1823A[1] and associated mh1823[2] software address NDE POD testing for two types of datasets. The first type of dataset is that of the signal response "$\hat{a}$" (read as a-hat) versus known flaw size "a". In analyzing such data, the $\hat{a}$ data is represented on the y-axis and the "a" data on the x-axis and the data may be transformed using a logarithmic function, if needed, to provide a linear relationship around the signal response decision threshold level. A generalized linear model (GLM) is fitted to the data using maximum likelihood estimate (MLE) for analysis. In this analysis, noise data, defined as the signal response in a region where there is no flaw, is also obtained. The noise data is used to estimate false call rate or probability of false positive calls (POF).

The second type of dataset considered is that of hit-miss data, which contains the known flaw sizes and the corresponding detection results i.e., hits or misses. For numerical analysis, a hit is assigned a numerical value of 1 while a miss has numerical value of 0. False call data (i.e., a hit is called where no flaw exists) is also recorded and used to determine the POF using the Clopper-Pearson binomial distribution function. Typically, POD increases with increasing flaw size and POF decreases with increasing flaw size. POF shall be required to be less than a certain limit to prevent adverse impacts on cost and schedule necessary to take corrective actions to address the false positive calls. ASTM E2862[3] also provides a hit-miss POD data analysis method that is consistent with MIL-HDBK-1823A. There are other POD analysis approaches that are not covered by MIL-HDBK-1823A. The Binomial point estimate method of verifying reliably detectable flaw size is given by Rummel[4].

Current work is in probability of detection (POD) analysis using tolerance intervals[5,6]. This work is limited to POD analysis and simulation approach for single-hit limited sample POD[7] or LS POD. Broadly, LS POD covers signal response-based data for both single-hit and multi-hit POD applications including modeling of transfer functions[7-15]. Smaller sample size is usable in LS POD analysis. In practice, signal responses from smaller sample size of flaws may not be random to the population. LS POD assumes that the sample is randomly drawn from the population or is conservative to the population. Generally, a sample is drawn from one end of the signal response population where average and standard deviation of signal responses are assumed to be lower than that of the population. These samples are conservative and are called worst case signal responses[9]. Koshti[10,16] provides model for transfer function method using linear fit to data. Transfer function model is used to qualify or validate NDE procedure in detecting flaws reliably. NESC Guidebook[16] provides guidelines for implementation of the transfer function method for both forward and inverse cases and provides extensive list of relevant references. Transfer function analysis method using user provided data is also provided here. Koshti[17] provides transfer function signal response relationships model and uses it to define transfer function approach for qualifying NDE procedure. Saturating signal response is used in the model. The transfer function method uses either a linear or second order polynomial fit to signal response data. A method of transfer function sensitivity analysis using simulated data is provided.

2. SIGNAL RESPONSE TRANSFER FUNCTION DATASET VRIABLE BLOCKS

A case of detection of induced embedded flaws using a signal response based NDE method such as eddy current is considered. It is assumed that induced embedded flaw specimens will not be available. Here, the objective is to qualify an NDE signal response-based flaw detection technique for detecting natural or induced flaws similar to embedded flaws or flaws that cannot be fabricated with controlled geometry and size. Goal of the qualification is to determine a reliably detectable embedded flaw size denoted as $a_{90/95}$ with estimated P/C (POD/Conf.) of 90/95% based on transfer function model. Embedded flaw detection is also referred to as volumetric inspection. In absence of specimens with such flaws, a purely empirical method of qualification would not work. It is assumed that a physics-model based signal response versus flaw size simulation is available for the desired flaw-material characteristics. This approach uses simulated and empirical signal response data to construct the transfer function qualification model. Induced and machined surface flaws are used in NDE procedure qualification. NDE signal response can be simulated for both embedded and surface flaws.

Transfer function between simulated and empirical signal response data of surface flaw signal response will be used in the model. Once, simulated signal response data for surface flaws is correlated using empirical data, it is assumed that same correlation exists for signal response data for the embedded flaw. This assumption should be carefully handled, making sure that correlation coefficient is high in the relevant range of flaw sizes and difference in embedded flaw signal response from the corresponding surface flaw signal response is within a small percentage. Here, physics-model based simulation would be used to simulate signal response from same size and geometry surface breaking and embedded flaws. Relationship between two signal responses would be used in this model.

A single step transfer function uses two flaw attributes (e.g., part geometry and flaw location) each of which has two (binary) values. See Table 1. This is described as 2 flaw attributes x 2 values transfer function case. This case results in 4 signal response versus flaw size functions i.e., $y = f(x)$ variable relationships (characteristics or datasets). Three signal response functions are used as input and fourth is estimated based on first three signal response inputs. Any 2 x 2 transfer function block defines 2 transfer functions. The set of four signal response functions can be described as a transfer variable block as certain relationships are assumed between these functions, allowing transfer function analysis within the block. A general transfer function approach is to design the 2 x2 transfer function block or blocks and create a sequence of data block calculations. The sequence should be such that output from earlier data block calculations may be used as input in later data block calculations leading to the desired estimation of signal response characteristics.

"x" is used to denote the variable for flaw size and "y" is used to denote dependent variable or function corresponding to signal response in each dataset. There are three flaw attributes in the current transfer function application. They are used as subscripts of "x" and "y" variables. For example, a single datapoint in a signal response dataset is denoted by a pair of variables as $(x_{flaw\ type, part\ geometry, flaw\ location}, y_{flaw\ type, part\ geometry, flaw\ location})$. Signal response variable or data type is also numbered from Dataset 1 through Dataset 8 for simplicity. Signal response relationships model will be defined before explaining transfer function approach or models. Legend for the subscripts is given in Table 1. First column attribute (flaw type) has three values. Therefore, this flaw attribute is ternary. Second and third column attributes (part geometry and flaw location) have two values each. These attributes are binary.

Table 1: Subscript convention for variables “x” and “y”

Flaw Type (Ternary)	**Part Geometry (Binary)**	**Flaw Location (Binary)**
e – artificial, machined, or Machined flaw	1 – simple geometry	1 – location 1 e.g., surface
c – induced or cracklike flaw	2 – part geometry	2 – location 2e.g., embedded
s – computer simulated flaw		

Selected datasets are numbered from 1 through 8. See Table 2. Out of 8 signal response datasets (or variables), three input datasets are gathered as empirical data and two input datasets are gathered as physics-model based simulation data. Datasets 1, 2, and 3 are empirical datasets. Datasets 5 and 6 are gathered by physics-model based simulation exercise. Datasets 4, 7, and 8 are calculated or derived from other datasets. Objective of the transfer function dataset relationship model is to estimate Dataset 8 $y = f(x)$ characteristics (i.e., mean $\bar{y}$ and lower 90/95 P/C $y_{90/95,lower}$).

The datasets are divided in three blocks i.e., Block 1, 2, and 3 of four datasets each. In each block, the bottom right dataset is computed from the other three datasets. Therefore, the blocks are called signal response transfer variable blocks. Process of computation is identical within each block. The variable relationships may be similar between blocks. Output of Block 1 i.e., Dataset 4 is useful for determining POD flaw size for induced surface flaws. Output of Block 1 is not used in other two blocks in Example 1. Output of Block 2 is used in Block 3. Therefore, this is a two-step or block transfer function approach. Three types of flaws (artificial, induced and simulated) are used in this application. Other two flaw attributes (part geometry and location) have two values each. Therefore, this transfer function can have a maximum of 2 x 2 x 3 or 12 signal response variables. Only 5 input datasets and 2 or 3 output datasets are used. The transfer function in mapped in two 2 x 2 signal response variable blocks (i.e., Block 2 and Block 3). The simulated signal responses i.e., Dataset 5 and Dataset 6 must show a strong correlation. Moreover, Dataset 2 and Dataset 5 shall a show strong correlation.

Table 2: Signal response variables for datasets and transfer variable blocks. Dataset blocks Example 1

Block	**Specimen Geometry**	**Location**	**Flaw Type**	
1			**Machined Flaw**	**Induced Flaw**
	Simple Geometry, 1	Surface, 1	Dataset 1: $y_{e,1,1}$or	Dataset 3: $y_{c,1,1}$
	Part Geometry, 2	Surface, 1	Dataset 2: $y_{e,2,1}$	Dataset 4: $y_{c,2,1}$(output 1)
2			**Computer Simulated Flaw**	**Machined Flaw**
	Part Geometry, 2	Surface, 1	Dataset 5: $y_{s,2,1}$	Dataset 2: $y_{e,2,1}$
	Part Geometry, 2	Embedded, 2	Dataset 6: $y_{s,2,2}$	Dataset 7: $y_{e,2,2}$ (intermediate output 2)
3			**Machined Flaw**	**Induced Flaw**
	Simple Geometry, 1	Surface, 1	Dataset 1: $y_{e,1,1}$	Dataset 3: $y_{c,1,1}$
	Part Geometry, 2	Embedded 2	Dataset 7: $y_{e,2,2}$	Dataset 8: $y_{c,2,2}$(output 3)

The signal response variable can be named generically by two subscripts as given in Table 3 by a block number and a block variable number. Each block has four signal response variables numbered from 1 through 4. Generic variable subscript is “vn,bn”, where number to the right of “v”, given by “n”, is a variable number which is between 1 to 4, and “number to the right of “b”, given by “n” is the block number. There are two binary flaw attributes and one ternary flaw attribute for the variables in Example 1. In each block, variable 4 is computed in more or less same way using the three corresponding block variables. This allows for setting up similar computation routines between the variable blocks. As observed in Table 2, some of the variables from one block are used in another block. For example, Block 1 Dataset 1: $y_{v1,\mathrm{b}1}$ is same as Block 3 Dataset 1: $y_{v1,b3}$. Purpose of providing a generic block variable table is to emphasize that the two or more transfer variable blocks may be set-up in different ways depending upon transfer function application. The first step in transfer function approach is to create 2 x 2 transfer function variable blocks. Table 3 provides an Example 2 with different flaw attributes with generic notation but is similar to Example 1.

Intermediate output (or a derived variable) from Block 2 is used in Block 3. Here, any input variables of Block 2 cannot be reused in Block 3 to maintain independence of input variables. Block 2 calculation will be performed first, and Block 3 calculation is performed last. The block input variables shall be independent. When derived variables are used as an input, along with other input variables, the derived variables as well as other input variables should be independent.

Table 3: Generic transfer function block variable notation. Dataset blocks Example 2.

Block	**Binary Feature A (Geometry)**	**Binary Feature B (Location)**	**Ternary Feature C (Flaw Type)**	
1			**1** (EDM notch)	**2** (Induced crack)
	1 (Tube OD, no weld)	**1** (ID surface)	Dataset 1: $y_{v1,\mathrm{b}1}$or	Dataset 3: $y_{v3,b1}$
	2 (Tube OD, weld)	**1** (ID surface)	Dataset 2: $y_{v2,b1}$	Dataset 4: $y_{v4,b1}$(Output 1)
2			**3** (Simulated flaw)	**1** (EDM notch)
	2 (Tube OD, weld)	**1** (ID surface)	Dataset 5: $y_{v1,b2}$	Dataset 2: $y_{v3,b2}$
	2 (Tube OD, weld)	**2** (Embedded close to ID)	Dataset 6: $y_{v2,b2}$	Dataset 7: $y_{v4,b2}$ (output 2)
3			**1** (EDM Notch)	**2** (Induced Crack)
	1 (Tube OD, no weld)	**1** (ID surface)	Dataset 1: $y_{v1,b3}$	Dataset 3: $y_{v3,b3}$
	2 (Tube OD, weld)	**2** (Embedded close to ID)	Dataset 7: $y_{v2,b3}$	Dataset 8: $y_{v4,b3}$ (Output 3)

In Example 3, only two dataset variable blocks are used. Dataset 7 is not computed.

Table 4: Dataset blocks Example 3

Block	**Specimen Geometry**	**Location**	**Flaw Type**	
1			**Machined Flaw**	**Induced Flaw**
	Simple Geometry, 1	Surface, 1	Dataset 1: $y_{e,1,1}$or	Dataset 3: $y_{c,1,1}$
	Part Geometry, 2	Surface, 1	Dataset 2: $y_{e,2,1}$	Dataset 4: $y_{c,2,1}$(output 1)
2			**Computer Simulated Flaw**	**Induced Flaw**
	Part Geometry, 2	Surface, 1	Dataset 5: $y_{s,2,1}$	Dataset 4: $y_{c,2,1}$
	Part Geometry, 2	Embedded, 2	Dataset 6: $y_{s,2,2}$	Dataset 8: $y_{c,2,2}$(output 3)

When constructing dataset blocks, it is important to justify the assumed relationship between the variables. If the relationships cannot be justified, then the respective block calculations cannot be justified. Dataset blocks Example 4 is provided with slightly different subscript convention. It is more applicable for transfer between instrument set-ups.

Table 4: Signal response variables for datasets and transfer variable blocks. Dataset blocks Example 4.

	Set-up	**Location**	**Flaw Type**	
1			**EDM Notch (en)**	**Fatigue Crack (fc)**
	Set-up 1 (s1)	Flat Farside (g1)	Dataset 1: $y_{en,g1,s1}$	Dataset 3: $y_{fc,g1,s1}$
	Set-up 1 (s1)	I.D. (g2)	Dataset 2: $y_{en,g2,s1}$	Dataset 4: $y_{fc,g2,s1}$ (Output 1)
2			**Computer Simulated Notch (cn),**	**EDM Notch (en)**
	Set-up 1 (s1)	I.D. (g2)	Dataset 5: $y_{cn,g2,s1}$	Dataset 2: $y_{en,g2,s1}$
	Set-up 2 (s2)	I.D. (g2)	Dataset 6: $y_{cn,g2,s2}$	Dataset 7:$y_{en,g2,s2}$ (output 2)
3			**EDM Notch (en)**	**Fatigue Crack (fc)**
	Set-up 1 (s1)	Flat Farside (g1)	Dataset 1: $y_{en,g1,s1}$	Dataset 3: $y_{fc,g1,s1}$
	Set-up 2 (s2)	I.D. (g2)	Dataset 7: $y_{en,g2,s2}$	Dataset 8: $y_{fc,g2,s2}$(output 3)

Dataset blocks Example 4 is identical to dataset blocks Example 1 and 2 from mathematical modelling point of view. The dataset variable names i.e., Dataset 1 through 8 are same. Data attributes and interpretation are different. There is a noise distribution corresponding to each empirical dataset. Noise distribution is affected by part geometry but also by the set-up. Therefore, noise distributions may be different between set-up 1 and set-up 2. Threshold level noise level corresponding to probability of false positive (POF) denoted as $y_{fc,g2,s2}^{POF,1/95}$ (i.e., 1 %POF and 95% confidence) may be computed. Noise measurements should be in unflawed areas where flaw could occur. The decision threshold $y_{fc,g2,s2}^{thr}$ should be greater than or equal to noise threshold and less than or equal to the 90/95 P/C signal level $y_{fc,g2,s2}^{POD,90/95}$. In above Example, a method is provided to use Dataset 7 for calibration (instrument standardization). The method uses Block 3 transfer function to calculate $y_{fc,g2,s2}^{POD,90/95}$. A decision threshold is chosen such that $y_{fc,g2,s2}^{POF,1/95} \leq y_{fc,g2,s2}^{thr} \leq y_{fc,g2,s2}^{POD,90/95}$.

3. SIGNAL RESPONSE TRANSFER RELATIONSHIPS MODEL FOR EXAMPLE 1

Only variables and blocks of Example 1 (Table 2) will be considered in rest of the paper to illustrate the transfer function approach with simulated data. An Example of simulated data for signal response transfer relationships model is provided in Fig. 1. Fig. 1 datasets use a model similar to a model used by Koshti[17]. Dataset 8 is the desired result of transfer function computation and is shown in the Fig. 1 bottom plot as Data 8.

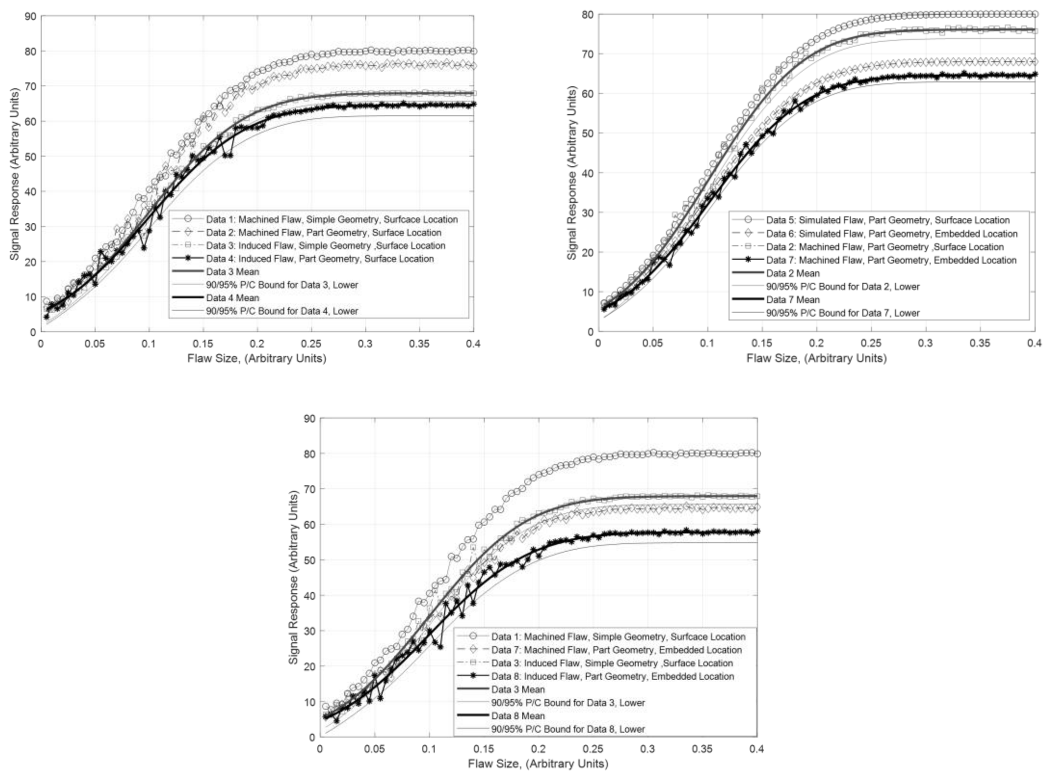

Fig. 1: An example of simulated data for signal response transfer relationships model. Top left: Block 1, top right: Block 2, and bottom: Block 3.

Output Datasets 4, 7 and 8 are computed using input datasets as given in Block 1, 2 and 3 respectively. If datapoints in appropriate flaw range and spacing for input block datasets are available, then output datasets can be computed.

Signal response saturation is quite common in NDE. Fig. 1 datasets have an upper and lower saturation limit. The data functions are modeled using an error function. However, parameters of this function can be chosen such that signal response will be approximately linear in the flaw range of interest. The transfer function model is developed for linear signal responses, therefore non-linearity in signal responses will impose limits on applicability of the transfer function model presented here. Signal response variation increases with flaw size but reduces as signal value approaches the saturation limit. This feature is modeled in this simulation as it may be observed in practice. Although, this feature may be suppressed in the signal relationships model. The results of signal response relationships model are applicable for similar datasets where signal response increases monotonically with flaw size to a limit.

Table 5: Block 1 signal response variables for Example 1

Block	**Specimen Geometry**	**Location**	**Flaw Type**	
1			**Machined Flaw**	**Induced Flaw**
	Simple Geometry, 1	Surface, 1	Dataset 1: $y_{e,1,1}$	Dataset 3: $y_{c,1,1}$
	Part Geometry, 2	Surface, 1	Dataset 2: $y_{e,2,1}$	Dataset 4: $y_{c,2,1}$(output 1)

Following mean signal response relationship is assumed,

$$\bar{y}_{c,2,1} = \frac{\bar{y}_{c,1,1}\bar{y}_{e,2,1}}{\bar{y}_{e,1,1}}, \tag{1}$$

where, $\bar{\ }$ is used to indicate mean value of dataset variable y at any given value of x. Here, standard deviation is assumed to be a function of flaw size. This equation is sometimes referred to as transfer ratio. The model assumes square root of the sum of squares formula for resulting standard deviation,

$$\sigma^x_{c,2,1} = \sqrt{\left(\sigma^x_{c,1,1}\right)^2 + \left(\sigma^x_{e,2,1}\right)^2 + \left(\sigma^x_{e,1,1}\right)^2} \tag{2}$$

or a more stringent relationship,

$$\sigma^x_{c,2,1} = \frac{\sigma^x_{c,1,1}\sigma^x_{e,2,1}}{\sigma^x_{e,1,1}}, \text{ if } \sigma^x_{e,1,1} \neq 0 \quad \text{and} \quad \sigma^x_{c,2,1} \cong \sigma^x_{c,1,1}, \quad \text{if } \sigma^x_{e,1,1} = 0 \tag{3}$$

Eq. (3) is an assumption that needs to be verified. Eq. (2) does not assume relationship between standard deviations other than that the input standard deviations, i.e., quantities in right hand side of Eq. (2) are independent. Eq. (1) assumes relationship between mean values of signal response. These are basic assumptions of the transfer response relationships for Block 1. In Fig. 1, error function fits are shown for Dataset 3 and Dataset 4 along with 90% lower data bound (for probability) with 95% confidence i.e., lower 90/95% P/C. It should be remembered that the fit and bounds are influenced by the selected data range. The saturating portion of the data may bring the data bounds closer, indicating that more datapoints are outside the middle portion of the curve. Thus, statistical curve fitting to assess confidence bounds may have limitations if signal response variance is also a function of the flaw size. Eq. (1) and Eq. (2) (or Eq. (3)) describe a chosen signal response variable relationships completely for Block 1.

Here, Block 2 is designed for using the simulated flaw response for surface and embedded flaws. See Table 7A.

Table 7A: Block 2 signal response variables for Example 1, part geometry only

Block	**Specimen Geometry**	**Location**	**Flaw Type**	
2			**Computer Simulated Flaw**	**Machined Flaw**
	Part Geometry, 2	Surface, 1	Dataset 5: $y_{s,2,1}$	Dataset 2: $y_{e,2,1}$
	Part Geometry, 2	Embedded, 2	Dataset 6: $y_{s,2,2}$	Dataset 7: $y_{e,2,2}$ (intermediate output 2)

Some equations are repeated as they are necessary to describe the block variable relationships. Following mean signal response relationship is assumed,

$$\bar{y}_{e,2,2} = \frac{\bar{y}_{s,2,2}\bar{y}_{e,2,1}}{\bar{y}_{s,2,1}}. \tag{4}$$

The model assumes square root of the sum of squares formula for resulting standard deviation,

$$\sigma^x_{e,2,2} = \sqrt{\left(\sigma^x_{s,2,2}\right)^2 + \left(\sigma^x_{e,2,1}\right)^2 + \left(\sigma^x_{s,2,1}\right)^2} \qquad \text{where } \sigma^x_{s,2,1} = \sigma^x_{s,2,2} = 0 \tag{5}$$

$$\sigma^x_{e,2,2} \cong \sigma^x_{e,2,1} \tag{6}$$

These are basic assumptions for the transfer response relationships for Block 2. Block 3 variable and variable relationships are defined below.

Table 8A: Block 3 signal response variables for Example 1 datasets

Block	Specimen Geometry	Location	Flaw Type	
3			**Machined Flaw**	**Induced Flaw**
	Simple Geometry, 1	Surface, 1	Dataset 1: $y_{e,1,1}$	Dataset 3: $y_{c,1,1}$
	Part Geometry, 2	Embedded 2	Dataset 7: $y_{e,2,2}$	Dataset 8: $y_{c,2,2}$(output 3)

Following mean signal response relationship is assumed,

$$\bar{y}_{c,2,2} = \frac{\bar{y}_{c,1,1}\bar{y}_{e,2,2}}{\bar{y}_{e,1,1}}. \tag{7}$$

The model assumes square root of the sum of squares formula for resulting standard deviation,

$$\sigma^x_{c,2,2} = \sqrt{\left(\sigma^x_{c,1,1}\right)^2 + \left(\sigma^x_{e,2,2}\right)^2 + \left(\sigma^x_{e,1,1}\right)^2}. \tag{8}$$

or a more stringent relationship,

$$\sigma^x_{c,2,2} = \frac{\sigma^x_{c,1,1}\sigma^x_{e,2,2}}{\sigma^x_{e,1,1}} \text{ if } \sigma^x_{e,1,1} \neq 0, \text{ and } \quad \sigma^x_{c,2,2} \cong \sigma^x_{c,1,1}, \quad \text{if } \sigma^x_{e,1,1} = 0 \tag{9}$$

4. DESCRIPTION OF FORWARD AND INVERSE CASES FOR TRANSFER FUNCTION

Desired output of transfer function calculations may be a single value or a dataset. For computing the output variable characteristics, transfer variable relationships, as given in Eq. (1) through Eq. (9), would be adequate. Generally, single value calculation propagates error at the point of calculation and may be more conservative than using square root of the sum of squares formula (e.g., Eq. (2)) for every datapoint. If signal response characteristics in a desired range is computed for the output datasets, then a one can choose a threshold level and interpolate flaw sizes at the threshold level for desired datasets. If two or more blocks are used in the transfer function calculation, the intermediate output variable characteristics should be defined in the relevant range of flaw sizes. It is assumed that the three input data characteristics are known in a given variables block for a relevant flaw size range. Using this assumption, an example of forward and inverse case is considered for Block 1 of Example 1. If the desired output is a single value, then the last computation block can follow the following steps.

For forward case of transfer function in Block 1 of Example 1, a target flaw size to be detected reliably in the part, denoted as $x^{target,F}_{c,2,2,90/95}$ is provided. Here, objective is to determine demonstration flaw size $y^{demo}_{c,1,1,90/95}$ for simple geometry specimens. Once the demonstration flaw size is known, a demonstration test can be set-up to test operators using Binomial point estimate method or LS POD[15] method. Alternately, a range of flaws containing the demonstration flaw size can be manufactured and used in the operator demonstration test using MIL-HDBK-1823 POD analysis methods. If the operator demonstrates minimum 90/95% P/C to detect the demonstration size flaw, then the operator is assumed to have demonstrated high reliability in detecting the target size flaw in the part. The operator also needs to supplement the demonstration by detecting relevant same size flaws belonging to Dataset 2 type. This will verify that the NDE procedure provides acceptable flaw detectability in part geometry specimens. Thus, the forward transfer method is used to qualify a flaw size for NDE procedure demonstration using induced flaws in simple geometry specimens.

For inverse case, induced flaw size $y^{demo}_{c,1,1,90/95}$ with 90/95% P/C for demonstration in simple geometry specimens is known. Here, objective is to determine smallest reliably detectable flaw size in part i.e., $x^{est}_{c,2,2,90/95}$ using the NDE procedure at hand. Here, the exact procedure that was used in the demonstration may not be known, but it is assumed that the NDE procedure used in demonstration is similar to the procedure under evaluation. The procedure under evaluation is assumed to be equivalent or better in terms of flaw detectability compared to the one used in the demonstration.

Generally, there is a fracture control requirement to detect a flaw size with minimum 90/95% P/C. Here, this flaw size is denoted by $a^{req}_{c,2,2,90/95}$. Both forward and inverse transfer functions are used in relation to this flaw size such that the NDE procedure qualified flaw size should be smaller than the requirement flaw size. It should be remembered that determining smallest reliably detectable flaw size (inverse case) or 90/95% P/C demonstration flaw size for a given target flaw size (forward case) do not provide P/C of 90/95% directly due to a number of assumptions and use of intermediate estimations such as for dataset 7. The transfer function method can provide $y^{demo}_{c,1,1,90/95}$ or $x^{est}_{c,2,2,90/95}$ flaw size estimates based on acceptance of risk in using the signal response transfer relationships model and transfer function models.

5. FORWARD TRANSFER FUNCTION MODELS FOR BLOCK 1

Here the model is given for Block 3. The same model is used for Block 1 and 2 or for any similarly constructed blocks. For forward case Block 3 calculations should be performed after Block 2 output calculations of Dataset 7. Since samples of Dataset 1, Dataset 3 and Dataset 7 are used in transfer function, Eq. (1) is interpreted as follows for both forward and inverse models,

$$\bar{y}^{fit}_{c,2,2} = \frac{\bar{y}^{fit}_{c,1,1}\bar{y}^{fit}_{e,2,2}}{\bar{y}^{fit}_{e,1,1}}. \tag{10}$$

The superscript "fit" indicates that the data comes from fitted curves. Forward case calculation follows calculations in a sequence from point A to point F i.e., point A ---> point B ---> point C ---> point D ---> point E ---> point F in Fig. 2. Uncertainty in flaw size at each point of calculation is used to calculate compound uncertainty in the resulting calculation.

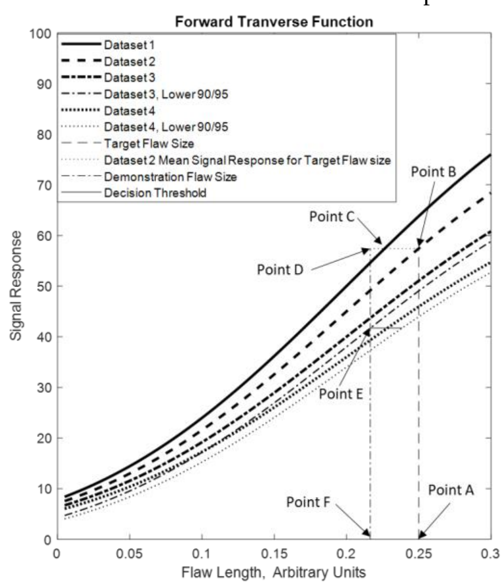

Fig. 2: Illustration of sequence of forward transfer function calculations

Using x-coordinate $x^{target,F}_{c,2,2}$ of point A, point B y-coordinate or signal response of point B (on Dataset 7 curve) is calculated as follows,

$$y^{mean,target}_{e,2,2} = interp\left(x, y^{fit}_{e,2,2}, x^{target,F}_{c,2,2}\right), \tag{11}$$

Where, *interp* = interpolation function. First two variables are linear arrays defining the fit curve while the third variable has a single value. Uncertainty in x-coordinate or flaw size, which is equivalent to uncertainty in y-coordinate at point B, is calculated as,

$$\Delta x^{target,F}_{e,2,2} = interp\left(y^{95C}_{e,2,1}, x, y^{mean,target}_{e,2,2}\right) - x^{mean,target}_{e,2,2} \ . \tag{12}$$

$y_{e,2,2}^{95C}$ is a curve for 95% lower confidence bound to Dataset 7 $y_{e,2,2}^{fit}$ curve. Next, x-coordinate or flaw size of point C (on Dataset 1 curve) is calculated as follows,

$$x_{e,1,1}^{mean,target} = interp\left(y_{e,1,1}^{fit} x, y_{e,2,2}^{mean,target}\right). \tag{13}$$

Uncertainty in x-coordinate or flaw size which is equivalent to uncertainty in y-coordinate at point C is calculated as,

$$\Delta x_{e,1,1}^{target,F} = interp\left(y_{e,1,1}^{95C}, x, y_{e,2,2}^{mean,target}\right) - x_{e,1,1}^{mean,target}. \tag{14}$$

There is uncertainty in locating point E on Dataset 3 curve. This uncertainty is calculated using following two equations.

$$y_{c,1,1}^{mean,target} = interp\left(x, y_{c,1,1,}^{fit} x_{e,1,1}^{mean,target}\right), \text{ and} \tag{15}$$

$$\Delta x_{c,1,1}^{target,F} = interp\left(y_{c,1,1}^{95C}, x, y_{c,1,1}^{mean,target}\right) - x_{e,1,1}^{mean,target}. \tag{16}$$

Because of sequential calculation, uncertainty in x-coordinate of point B carries over and adds to uncertainty in x-coordinate of point C. Using central limits theorem, uncertainty at point C is given by,

$$\Delta x^{F} = \sqrt{\left(\Delta x_{e,1,1}^{target,F}\right)^2 + \left(\Delta x_{e,2,2}^{target,F}\right)^2 + \left(\Delta x_{c,1,1}^{target,F}\right)^2}. \tag{17}$$

However, Dataset 3 $y_{c,1,1}^{fit}$ and $y_{c,1,1}^{95C}$ may not be known and $\Delta x_{c,1,1}^{target,F}$ may be unknown. Also, in the initial evaluation, Dataset 3 may not be available at all and $y_{c,1,1}^{fit}$ and $y_{c,1,1}^{95C}$ cannot be estimated. In this case, an assumption as follows can be made,

$$\Delta x_{e,2,2}^{target,F} \leq \Delta x_{c,1,1}^{target,F}. \tag{18}$$

Using above condition, Eq. (17) simplifies to,

$$\Delta x^{F} \geq \sqrt{\left(\Delta x_{e,1,1}^{target,F}\right)^2 + 2\left(\Delta x_{e,2,2}^{target,F}\right)^2} \text{ for } \Delta x_{e,2,2}^{target,F} \leq \Delta x_{c,1,1}^{target,F}. \tag{19}$$

Demonstration flaw size $x_{c,1,1}^{demo,F}$ is calculated as follows,

$$x_{c,1,1}^{demo,F} = x_{e,1,1}^{mean,target} - \Delta x^{F}. \tag{20}$$

Depending upon whether an approximate or calculated value of Δx^{F} is used, the results and confidence in the results are affected. Value of Δx^{F} should be greater than the uncertainty in the estimation of $x_{c,1,1}^{demo,F}$. This is given by following condition,

$$\delta x_{lim,F} > \Delta x^{F}. \tag{21}$$

It should be remembered that the transfer function model may not work close to the saturation limits i.e., lower, and upper limits due to non-linearity in signal response. Therefore, it is important to run the simulation exercise to understand whether application of transfer function model and sampling regime is likely to be successful. The paper provides method to determine whether transfer function validation is necessary. If transfer function validation is deemed necessary, then designing specimens for Dataset 1 and Dataset 7 samples and Dataset 3 demonstration set is needed. Using signal response data from Dataset 1 and Dataset 7 samples and above equations, the forward transfer function analysis can be performed. Generally, the model should work well if data can be modeled with linear fits. Linear fit is not possible near saturation limits where it would be advisable to check effectivity of the model using simulation.

6. INVERSE TRANSFER FUNCTION MODEL FOR BLOCK 1

The inverse case calculation follows calculations in a sequence from point A to point F i.e., point A ---> point B ---> point C ---> point D ---> point E ---> point F in Fig. 3. Only Block 1 model is given as others are similar. For inverse case, Block 3 calculations should be performed after Block 2 calculations for calculating Dataset 7.

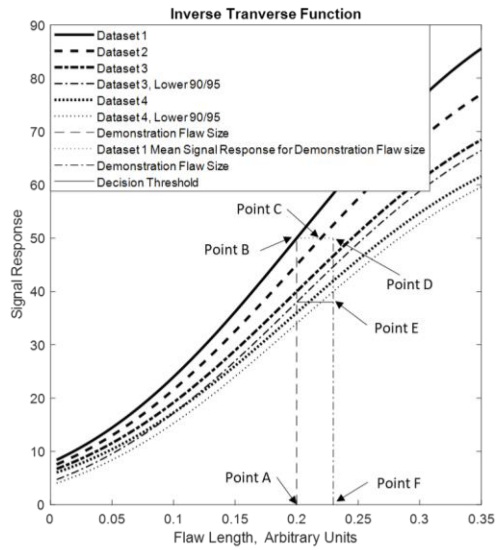

Fig. 3: Illustration of sequence of inverse transfer function calculations

Using x-coordinate of point A $x_{c,1,1}^{demo,I}$, point B y-coordinate or signal response (on Dataset 1 curve) is calculated as follows,

$$y_{e,1,1}^{mean,demo} = interp\left(x, y_{e,1,1}^{fit} x_{c,1,1}^{demo,I}\right). \tag{22}$$

Uncertainty in x-coordinate or flaw size, which is equivalent to uncertainty in y-coordinate at point B, is calculated as,

$$\Delta x_{e,1,1}^{demo,I} = interp\left(y_{e,1,1}^{95C}, x, y_{e,1,1}^{mean,demo}\right) - x_{c,1,1}^{demo,I} . \tag{23}$$

$y_{e,1,1}^{95C}$ is a curve for 95% lower confidence bound to Dataset 1 curve $y_{e,1,1}^{fit}$. Next x-coordinate or flaw size of point C (on Dataset 7 curve) is calculated as follows,

$$x_{e,2,2}^{mean,demo} = interp\left(y_{e,2,2}^{fit} x, y_{e,1,1}^{mean,demo}\right). \tag{24}$$

Uncertainty in x-coordinate or flaw size which is equivalent to uncertainty in y-coordinate at point C is calculated as,

$$\Delta x_{e,2,2}^{demo,I} = interp\left(y_{e,2,2}^{95C}, x, y_{e,1,1}^{mean,demo}\right) - x_{e,2,2}^{mean,demo}. \tag{25}$$

There is uncertainty $\Delta x_{c,1,1}^{demo,I}$ in locating the point A i.e., $x_{c,1,1}^{demo,I}$ on the Dataset 3 curve. It can be calculated using following two equations.

$$y_{c,1,1}^{mean,demo} = interp\left(x, y_{c,1,1}^{fit} x_{e,1,1}^{demo,I}\right), \text{ and} \tag{26}$$

$$\Delta x_{c,1,1}^{demo,I} = interp\left(y_{c,1,1}^{95C}, x, y_{c,1,1}^{mean,demo}\right) - y_{c,1,1}^{mean,demo}. \tag{27}$$

Because of sequential calculation, uncertainty in x-coordinate of point A carries over to and adds to uncertainty in x-coordinate of point B. Uncertainty in x-coordinate of point B carries over and adds to uncertainty x-coordinate of point C. Uncertainties in locating points A, B and C have effect on uncertainty in locating point E and this effect should be modeled using summation of quadrature of individual uncertainties using central limits theorem. Uncertainty at point E is given by,

$$\Delta x^{I} = \sqrt{\left(\Delta x_{e,1,1}^{demo,I}\right)^2 + \left(\Delta x_{e,2,2}^{demo,I}\right)^2 + \left(\Delta x_{c,1,1}^{demo,I}\right)^2} . \tag{28}$$

However, $y_{c,1,1}^{fit}$ and $y_{c,1,1}^{95C}$ may not be known and $\Delta x_{c,1,1}^{demo,I}$ may be unknown. The uncertainty $\Delta x_{c,1,1}^{demo,I}$ is included in $x_{c,1,1}^{demo,I}$ but value may not be known but it is recommended to add this uncertainty in the summation of quadrature of uncertainties. Incorporating $\Delta x_{c,1,1}^{demo,I}$ in Eq. (28) is more conservative. Dataset 3 may not be available at all and $y_{c,1,1}^{fit}$ and $y_{c,1,1}^{95C}$ cannot be estimated. In this case, an assumption as follows can be made,

$$\Delta x_{e,2,1}^{demo,I} \leq \Delta x_{c,1,1}^{demo,I}. \tag{29}$$

With above assumption, Eq. (28) is rewritten as,

$$\Delta x^{I} \ \geq \sqrt{\left(\Delta x_{e,1,}^{demo,I}\right)^{2} + 2\left(\Delta x_{e,2,2}^{demo,I}\right)^{2}} \text{ for } \Delta x_{e,2,2}^{demo,I} \leq \Delta x_{c,1,1}^{demo,I}. \tag{30}$$

Estimated reliably detectable flaw size $x_{c,2,2}^{est,I}$ is calculated as follows,

$$x_{c,2,2,90/95}^{est} = x_{e,2,2}^{mean,demo} + \Delta x^{I} \ . \tag{31}$$

Depending upon whether an approximate or calculated value of Δx^{I} is used, the results and confidence in results are affected. Value of Δx^{I} should be greater than the uncertainty in the estimation of $x_{c,2,2,90/95}^{est}$. This is given by following condition,

$$\delta x_{lim,I} > \ \Delta x^{I} \ . \tag{32}$$

Generally, the model should work well if data can be modeled with linear fit. Linear fit is not possible near saturation limits where it would be advisable to check effectivity of the model using simulation.

7. EXAMPLE OF FORWARD TRANSFER FUNCTION CALCULATIONS

Data processing example for forward transfer function model for dataset blocks Example 1 is provided. Figure 4 shows plots of example datasets. These are simulated datasets and are linear. Datasets 1 through 3 have replicates and there is data scatter in these datasets. Datasets 5 and 6 do not have replicates. They have smaller flaw size increment and do not have scatter. These datasets simulate data provided by the physics-based simulation.

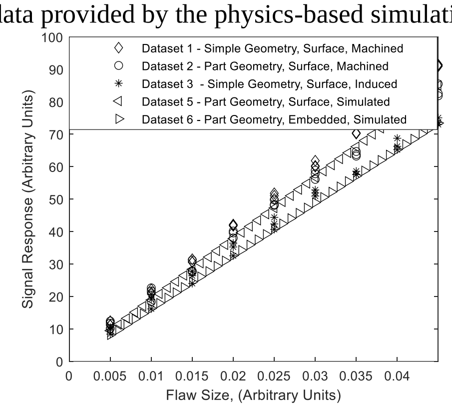

Fig. 4: Example datasets

Fig. 5 shows fitted function plots for datasets 1 and 2.

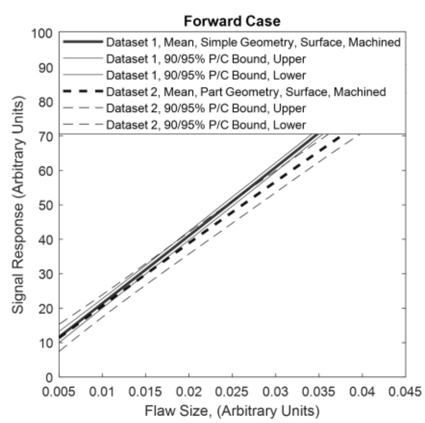

Fig. 5: Fitted function plots for datasets 1 and 2

Block 1 calculates demonstration flaw size.

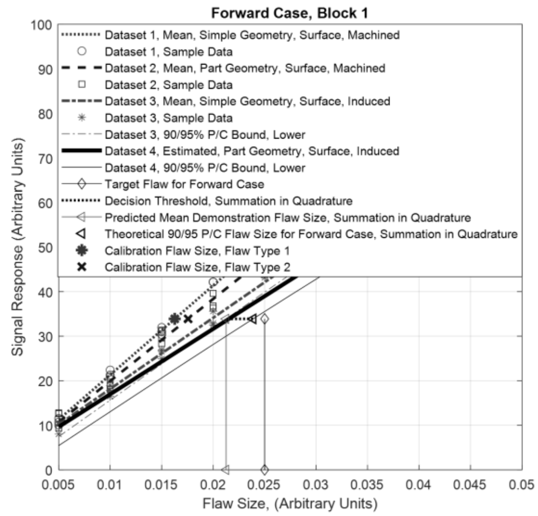

Fig. 6: Example of forward case for Block 1

Examples of forward and inverse case transfer function analysis is provided below. Here, simulated data is used as an input. Resulting flaw sizes for both forward and inverse case are calculated using Dataset 1 and Dataset 7 only. Eq. (44) is used for forward case and Eq. (55) is used for inverse case. However, Dataset 3 is shown in Fig. 8 and Fig. 10 for showing effectivity of the calculations. Both calculations seem to show approximately good results to Eq. (30) for forward case and to Eq. (32) for inverse case. Note that data is identical in Fig. 8 through Fig. 11.

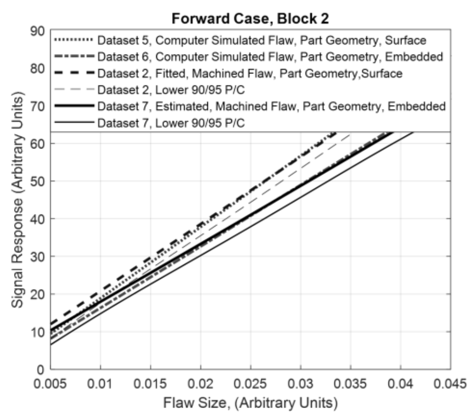

Fig. 7: Block 2 fitted datasets

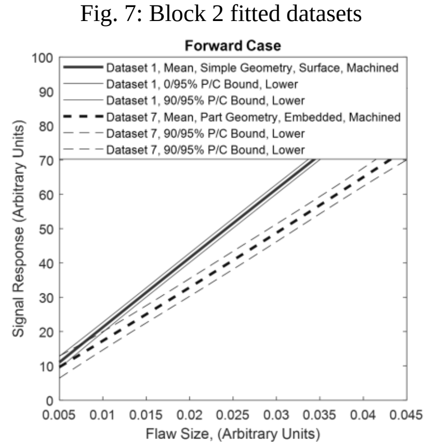

Fig. 8: Fitted datasets 1 and 7 for Block 3

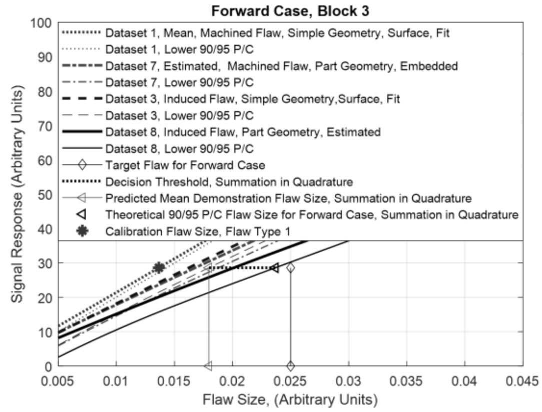

Fig. 9: Forward case for Block 3

8. EXAMPLE OF INVERSE TRANSFER FUNCTION CALCULATIONS

Data processing example for inverse transfer function model for dataset blocks Example 1 is provided. The example uses the same data as in previous section. Only, Block 1 and 3 charts are given below for inverse case. Block 2 chart is same between forward and inverse case.

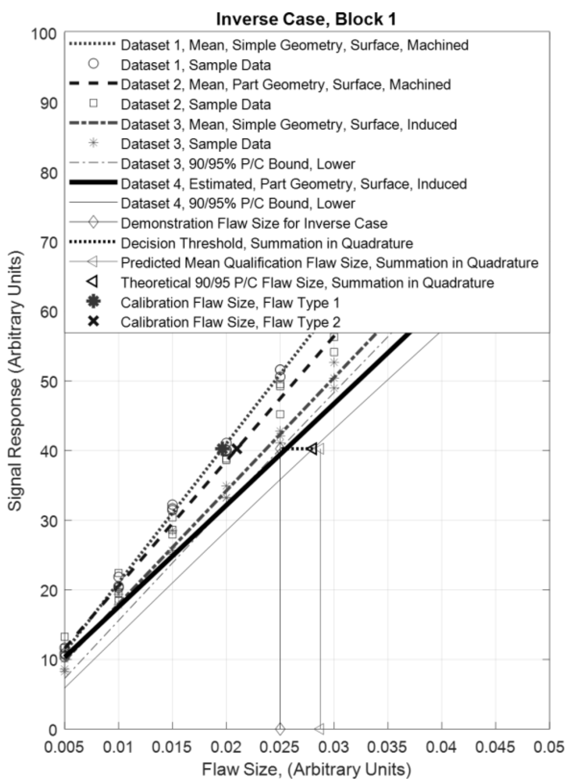

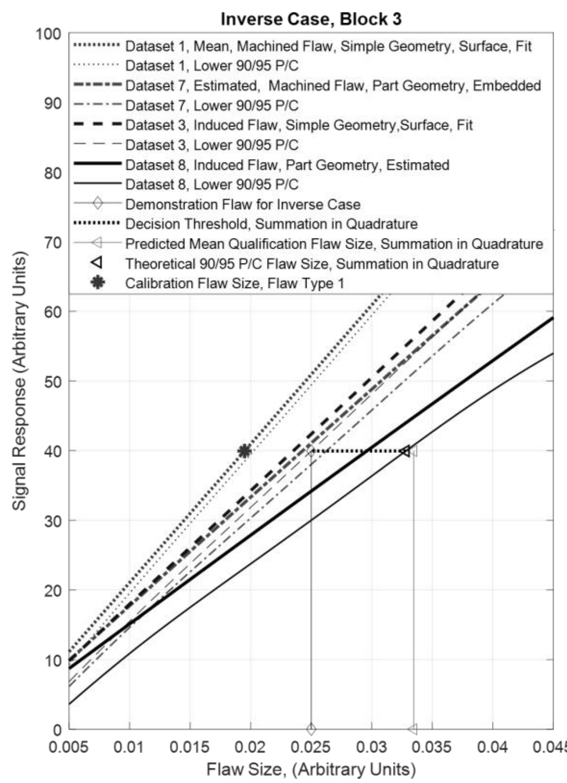

Fig. 10: Inverse case results for Block 1 and 3

9. CONCLUSIONS

The signal response transfer relationships model is devised first and then two step transfer function models have been devised for linear response signals with flaw size. The transfer function signal response relationships model provides relationship between these datasets towards estimating signal response from an embedded induced flaw. The transfer function model uses the signal relationships model to provide a model for calculating a signal decision threshold and corresponding 90/95% P/C flaw sizes. NDE procedure demonstration testing is performed on induced flaws in simple geometry specimens. An example of a transfer function NDE procedure qualification method for the forward and inverse cases is provided using simulated data. Another transfer function method, described as the inverse case, calculates the target flaw size using a given demonstration flaw size. Since, transfer function approach assumes signal relationships model, it is a risk assessment or indirect POD assessment approach. Both the signal response transfer relationships model and the transfer function model are important in managing risk in results provided by the transfer function NDE technique qualification or assessment. The signal response relationships model needs to be validated with empirical and simulation data and then transfer function model needs to be validated for desired P/C on case-by-case basis. If non-linearity is seen in the sampled data, a transfer function simulation method can be used to assess applicability and confidence in the transfer function method. Transfer function method may provide acceptable results for signal response data that can be modeled with linear fit. For non-linear data, transfer function simulation is advised to assess applicability of transfer function method. The transfer function method may be assessed using simulation to check whether the resulting target flaw size or demonstration flaw size provide adequate confidence to the assumed signal response transfer relationships model.

10. ACKNOWLEDGEMENTS

Dr. Samik Das (NASA JSC), and Nathan Trepal (NASA KSC) provided valuable review comments for this work.

REFERENCES

[1] MIL-HDBK-1823A, “Nondestructive Evaluation System Reliability Assessment,” Department of Defense, USA, (2009).

[2] Annis, Charles, “mh1823 POD Software V5.2.1,” Statistical Engineering, http://www.statisticalengineering.com/mh1823/, (2016).

[3] ASTM E 2862-12, “Standard Practice for Probability of Detection for Hit/Miss Dataset,” ASTM International, (2012).

[4] Rummel Ward D., “Recommended Practice for Demonstration of Nondestructive Evaluation (NDE) Reliability on Aircraft Production Parts,” Materials Evaluation, August Issue 40 pp 922, (1988).

[5] NIST/ Datasetplot, “SD Confidence Limits,” https://www.itl.nist.gov/div898/software/dataplot/refman1/auxillar/sdconfli.htm

[6] NIST/SEMATECH e-Handbook of Statistical Methods, Section 7.2.6.3, May 29, 2020, https://doi.org/10.18434/M32189, https://www.itl.nist.gov/div898/handbook/prc/section2/prc263.htm

[7] Koshti, Ajay M., “Using requirements on merit ratios for assessing reliability of NDE flaw detection,” SPIE Smart Structures and NDE, Proc. SPIE 11593, (2021).

[8] Koshti, Ajay M., “Using requirements on merit ratios for assessing reliability of NDE flaw detection in multi-hit detection in digital radiography,” SPIE Smart Structures and NDE, Proc. SPIE 11593, (2021).

[9] Koshti, Ajay M., "Assessing risk due to small sample size in probability of detection analysis using tolerance intervals," SPIE Smart Structures and NDE, Proc. SPIE 12048, Health Monitoring of Structural and Biological Systems XVI, 1204817 (2022).

[10] Koshti, Ajay M., “Assessment of flaw detectability using transfer function,” SPIE Smart Structures and NDE, Proc. SPIE 11592, (2021).

[11] Koshti, Ajay M., “Modeling reliability of an NDE method providing a C-scan, a case of flaw field simulation,” SPIE Smart Structures and NDE, Proc. SPIE 11593, (2021).

[12] Koshti, Ajay M., “Optimizing raster scanning parameters in nondestructive evaluation using simulation of probe sensitivity field,” SPIE Smart Structures and NDE, Proc. SPIE 11592, (2021).

[13] Koshti, Ajay M., “Assessing Visual and System Flaw Detectability in Nondestructive Evaluation,” SPIE Smart Structures and NDE, SPIE 11592, (2021).

[14] Koshti, Ajay M., “Probability of Detection Analysis in Multi-Hit Flaw Detection,” SPIE Smart Structures and NDE, SPIE 11594, (2021).

[15] Koshti Ajay, Parker Peter, Forsyth David, Suits, Michael, Walker James, and Prosser, William, “Guidebook for Limited Sample Probability of Detection (LS-POD) Demonstration for Single Hit Nondestructive Evaluation (NDE) Methods,” NASA Langley Research Center, NESC-TI-20-01545, (2021).

[16] Koshti Ajay, Parker Peter, Forsyth David, Suits, Michael, Walker James, and Prosser, William, "Guidebook for Assessing Similarity and Implementing Empirical Transfer Functions for Probability of Detection (POD) Demonstrations for Single-Hit Nondestructive Evaluation (NDE) Methods", NASA Langley Research Center, (2022).
[17] Koshti Ajay M., "Transfer function models and sensitivity analysis," SPIE Smart Structures and NDE, SPIE 12488, (2023).